Guidelines for Protection against Overcurrent in Photovoltaic Generators

Oscar GARCIA, Jesús-Casa HERNANDEZ, Francisco JURADO
Department of Electrical Engineering, University of Jaen, Paraje Lagunillas s/n, Jaen 23071, SPAIN
aquesada@ujaen.es, jcasa@ujaen.es, fjurado@ujaen.es

***Abstract*—This paper gives the scientific background and basic premises that should guide the design of overcurrent protection in photovoltaic generators (PVGs). Overcurrent protection first requires a thorough knowledge of potential risk scenarios and how to evaluate them. Accordingly, this paper describes electrical faults that may pose a risk to PVG because of overcurrents. It also evaluates these faults with a dynamic PVG model. This simulation model provides a realistic vision of the thermal and electrical behavior of the PVG from which implications of overcurrent protection can be drawn. A field test on a functioning 68-kWp PVG showed the accuracy of the simulation results regarding the risk of overcurrents, and validated the model used in our study. Within this context, this paper discusses how protective measures in the IEC 60364-4-43 can be applied to PVG. Since the measures in this standard were specifically conceived for alternating current low voltage (AC LV) systems, the unique operational characteristics of a PVG now make it necessary to revise and adapt them.**

***Index Terms*—electrical safety, fault currents, photovoltaic systems, protection, simulation.**

I. Introduction

PV systems have emerged as one of the most popular alternatives to conventional energy, thanks to technological advances and favorable government policies. However, there are still technical weaknesses that must be resolved. One of these weaknesses is the ineffectiveness of PVG operation under electrical fault conditions [1-2]. Electrical faults can seriously affect its safety [3].

The three main types of risk that affect safety in any electrical installation (e.g. PVG) are electric shock, overcurrent, and voltage disturbances [4]. Our previous studies on safety in PVGs were centered on protection from electric shock [5] and protection from voltage disturbances [6]. This paper completes our research on PVG safety by focusing on protection against overcurrent.

Overcurrent protection in PVGs has not been widely investigated. In the 1980s, references [7-8] described the practical problems that initially arose in the application of the National Electrical Code (NEC) [9] to PVGs. In the 1990s, Moechtar [10] first recommended the use of active means to detect overcurrents due to earth faults. References [11-12] proposed the use of fuses in PV strings as a means of protection. This proposal was reaffirmed by Laukamp [13-14] only if PVG had a high number of parallel-connected strings. Laukamp also pointed out that blocking diodes (BoDs) were unadvisable for overcurrent protection. Instead, he recommended an 'earth fault- and short-circuit proof' installation with class II PV modules (PVMs). Subsequent studies proposed double insulation as well as short-circuit and earth-fault tests as a means of preventing earth faults [15]. Finally, Wiles [16] underlined the fact that the NEC [9] requires the use of overcurrent protective devices (PDs) (e.g. fuses) in addition to a system for earth-fault protection in order to reduce fire risk. For some time now, various standards [17-18] have also claimed that BoDs are not reliable overcurrent PDs.

Similarly, PVG safety under electrical fault conditions is an issue that has rarely been addressed. Even though some researchers have studied the *I–V* and *P–V* characteristics of PVG under these conditions, very few [19] have experimentally obtained these characteristics by using an electronic load. Instead, most of them have used a model to simulate faulty conditions, in a specific PVG [20-25]. However, none of these models considered the combined effects of electrical faults and weather conditions (irradiance G, ambient temperature T_a, wind speed v_f) on the PV cell operating temperature (T_c), or on the PV cell's thermal dynamics. For this reason, we developed a dynamic model for PV devices [1-2], which is capable of dealing with varying weather conditions and also with the operation of any PVG under faulty conditions.

Overcurrent protection in conventional AC LV systems is regulated by the electrotechnical requirements defined in the IEC 60364-4-43 [26]. These requirements have evolved in consonance with technical knowledge and advances. PVGs are still in the initial stages of this process because this type of technology is relatively new, and also because its operational characteristics are unique [7-8], [12], [14], [27]. As part of the Univer Project [28], we analyzed the use of general protective measures for AC LV systems in PVGs, and found that it was difficult to apply many of these measures to PVGs precisely because of the way in which they operate. It was a fact that during the code-compliant design of overcurrent protection for the PVG, various difficulties were encountered in the interpretation of protection requirements if this protection was coordinated with electric shock protection [5] and lightning and surge protection [6]. This problem is also highlighted in [12-14], [29]. Although specific electrical codes [9], [18] and standards [17], [30] have moved to effect coverage of PV systems, there are still some practical problems that make the code difficult to apply.

II. Possible Electrical Faults in PVGs

Electrical faults in PVGs may be classified in two categories: short-circuit faults and open-circuit faults. A short-circuit fault can be defined as the unplanned occurrence of an accidental conductive path between one or

Digital Object Identifier 10.4316/AECE.2012.04010

more conductive parts and the earth (earth fault), or between two or more conductive parts of different electrical potential (phase-to-phase fault, Fig. 1). The conductive path is generally a short-circuit, i.e. fault resistance (R_{fault}) is zero. Earth faults are the most widespread in PVGs as reflected in the electrical failures discussed in the literature [7], [10], [11], [23]. Phase-to-phase faults occur inside a PVM or between PVMs of the same or of different module strings. The open-circuit fault is characterized by the interruption of one current-carrying part inside or outside a PVM.

The PVG can also develop unwanted conductive paths distributed throughout the PVG [31] (distributed earth fault).

III. Critical Observations under Electrical Fault Conditions

Using a simulation model developed in MATLAB/ Simulink® [1-2] we conducted a study on safety considerations in regards to overcurrents in a PVG (thermal stress) when the PVG operated under the electrical fault conditions described in section II. Our study was performed on a functioning 68-kWp PVG [28]. The parameters of the simulation model used for this PVG were the same ones as in [1-2]. This PVG consisted of 8 strings of 80 PVMs.

The model in [1-2] was improved to include distributed earth faults. For this purpose, the PVM insulation model [31] was taken into account. This model has a leakage capacitance $C_{lek\ mod}$, a series insulation resistance R_s, and a parallel insulation resistance R_p. These parameters are in direct relation to the insulation resistance and leakage capacitance of the PVG ($R_{iso\ G}$ and $C_{lek\ G}$) [31].

Subsequent simulations, unless otherwise specified, were performed at PVUSA Test Conditions (PTC) (G: 1000 W/m2; T_a: 20 ºC; v_f: 1m/s). Electricity variables (current i, voltage v, and power p) are normalized by their relevant values at Standard Test Conditions (STC) [1-2].

A. PVG Operating under a Short-Circuit Fault

1) Effect on module strings and PVG characteristics

To illustrate the effects of this fault type, firstly a fifty-module section of one of the PVG strings was short-circuited (Fig. 1(a)). We then analyzed a short-circuit between two strings, involving 50 PVMs (Fig. 1(b)). The following graphs only show results when BoDs were omitted, which is the worst case of thermal stress.

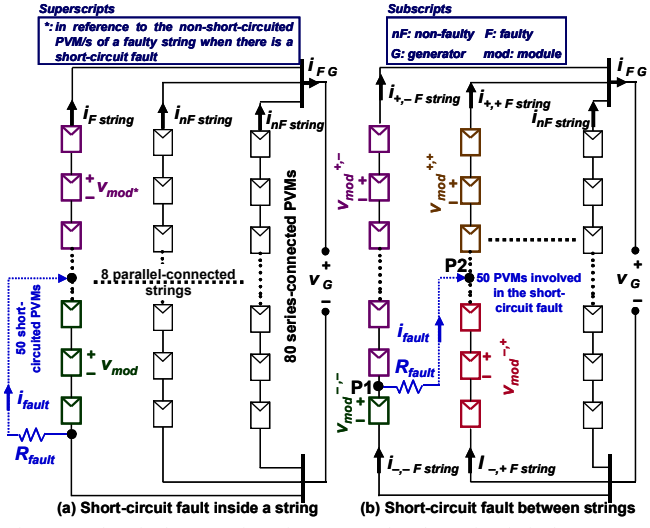

Figure 1. Electrical connections for PVG under short-circuit faults.

In the case of a short-circuit inside a string, Fig. 2 shows the i–v_G characteristics of the faulty string and of the normally operating strings as well as the PVG characteristics with and without the fault. The nomenclature used is reflected in Fig. 1(a). This graph also shows the p–v_G characteristics of the faulty/non-faulty PVG, along with the dissipated power and cell operating temperature in the PVMs* of the faulty string (variables p_c (PVM*) and T_c (PVM*)). Finally, the fault current i_{fault} and the time required so that temperature of solar cells of the PVM* reach its safety threshold (ST) ($T_{c\ ST}$=358 K) are likewise plotted. This time is called hereafter variable t_{SC}.

The short-circuit fault in a string led to a reduction of the voltage generated by the short-circuited section. Thus, the open-circuit voltage of the faulty string was reduced (0.89 to 0.33 p.u.), which was its most salient feature. The shape of the characteristic remained basically unchanged. This short-circuit with parallel strings led to a reverse current ($i_{F\ string}$ <0) through the PVMs* when the PVG voltage exceeded 0.33 p.u. (point A). From this point, the PVMs* were operated at voltages higher than their open-circuit voltage. Nonetheless, previously from point B, the generating capability of the faulty string was reduced, and as a result, the PVG current decreased.

Regarding p_c–v_G characteristics, the PVMs* became forward biased and dissipated power (p_c<0 p.u. –PVM*–) in the form of heat. This dissipated power increased their operating temperature (T_c –PVM*–) beyond its ST for high bias voltages. The worst case of thermal stress arose when the PVG was open-circuited, i.e. at Open-Circuit (OC) conditions. In this respect, 121s were necessary for the operating temperature of PV cells in PVMs* (T_c –PVM*–) to reach $T_{c\ ST}$, which increased from 48 ºC to well over 120ºC.

The heating of the PVMs* was dynamic. Thus, just after the short-circuit, the characteristics are denoted by superscripts +. As the PVM* heated up, its open-circuit voltage decreased (i. e. $i_{+F\ string}$–v_G characteristic → $i_{F\ string}$–v_G characteristic). As a result, the reverse current increased and the PVG open-circuit voltage decreased (i.e. $i_{+F\ G}$–v_G → $i_{F\ G}$–v_G) until thermal equilibrium was reached. For example, from the fault moment to the steady state, at OC conditions, the power dissipated in the PVMs* decreased slightly, more specifically, from point C (-15.95 p.u.) to point D (-14.01 p.u.).

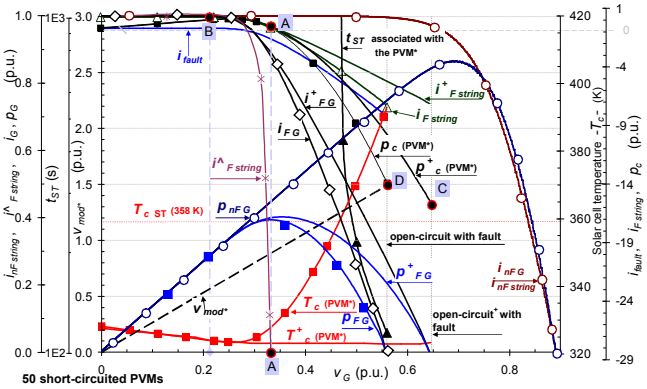

Figure 2. Simulation results for various characteristics in the functioning 68-kWp PVG (without BoDs) at PTC, with 50 PVMs short-circuited in a string.

In the case of a short-circuit between two strings, Fig. 3 depicts the same characteristics as Fig. 2. The nomenclature used is reflected in Fig. 1(b). After comparing Fig. 2 and 3, we concluded that the behavior of the faulty PVG in both cases was the same. Furthermore, PVMs belonging to the top side of the higher voltage point of the fault (mod+,+) and to the bottom side of the lower voltage point of the fault (mod–,–) behaved exactly the same as the PVMs* when the short-circuit occurred inside the string. Meanwhile, the i_{Fstring}–v_{G} characteristic of the PVMs, on the top side of the lower voltage point (mod+,–) and on the bottom side of the higher voltage point (mod–,+) varied with the position of the fault points. The first ranged from the characteristic of a non-faulty string (point *P1* bonded to the negative terminal) to a short-circuited string (point *P1* bonded to the positive terminal). The second behaved in exactly the opposite way. The results in Fig. 3 show that the lower voltage point is almost bonded to the negative terminal (only 1 PVM).

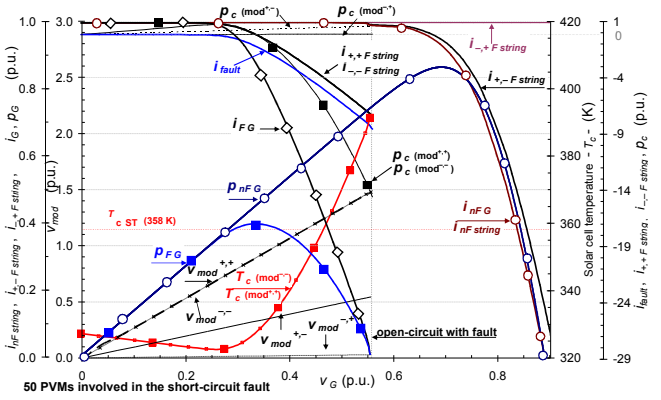

Figure 3. Simulation results for various characteristics in the functioning 68-kWp PVG (without BoDs) at PTC, with a short-circuit between two strings (involving 50 PVMs).

2) Relevance of the number of PVMs short-circuited

The number of PVMs short-circuited ($N_{\text{SC mod}}$ variable) had an important influence on the variation in dissipated power in the PVMs*, and therefore, on their operating temperature in a steady state. Fig. 4 illustrates thermal results at PTC for several short-circuit faults of increasing severity in a PVG string with and without BoDs. The $N_{\text{SC mod}}$ variable ranged from 0 to 79.

When the thermal results, with and without BoDs, were compared, the PVMs* were found to be more heavily loaded when there were no BoDs. BoDs thus avoided reverse currents and dissipated power. Thus, without BoDs, more than 29 short-circuited PVMS led to temperatures higher than $T_{\text{c ST}}$ in the PVMs* when the PVG was open-circuited. At this point, a 3.96 p.u. reverse current ($i_{\text{F string}}$) flowed through the PVMs* and a 6.50 p.u. power (p_{c} –PVM*–) was dissipated. As the $N_{\text{SC mod}}$ variable increased, the previous variables tended towards the following minimum values:

$$i_{F\ \text{string}} \rightarrow (N_{pa}-1); \qquad p_c \rightarrow v_{oc\ \text{mod}*} \times (N_{pa}-1) \qquad (1)$$

where N_{pa} is the number of parallel-connected strings in the PVG and $v_{\text{oc mod}}$ is the open circuit voltage of the PVM. These minimum values remained invariable when the variable $N_{\text{SC mod}}$ was greater than 60. When the PVG operated at Maximum Power Point (MPP) conditions, the PVMs* did not dissipate power.

Thermal stress in this fault condition, in addition to the $N_{\text{SC mod}}$ variable, were found to depend on weather conditions. In order to study the combined effect of all variables, the simulations in Fig. 4 were extended to several levels of irradiance (200–1200 W/m2, 100 W/m2 step) and ambient temperature (-10–40 ºC, 5 ºC step). Thus, for example, Fig. 5 shows the dissipated power in the PVMs* when the PVG was open-circuited. This dissipated power, mainly depended on irradiance. Nevertheless, the influence of the ambient temperature was very slight.

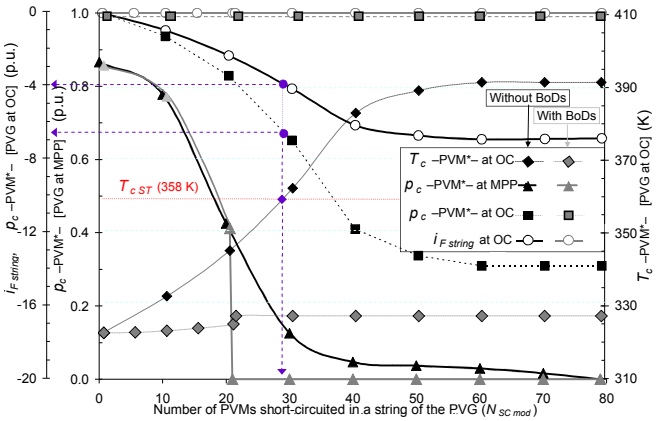

Figure 4. Thermal stress for the PVMs* in the functioning 68-kWp PVG, depending on NSC mod variable at PTC (MPP and OC conditions).

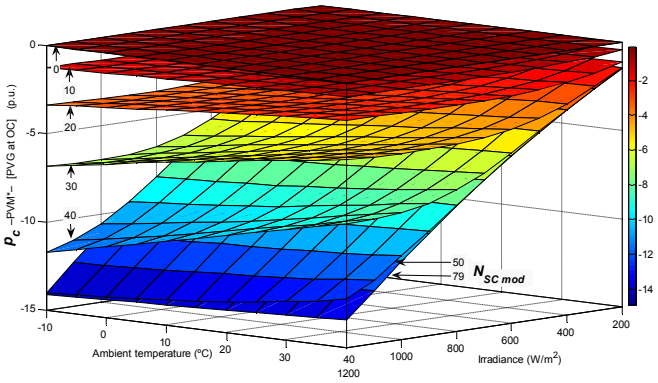

Figure 5. Dissipated power in the PVMs* when the functioning 68-kWp PVG was open-circuited (without BoDs and vf = 1 m/s).

3) Benefits of series/paralleling

Increasing the degree of parallelism in the PVG had an obvious effect on thermal stress. Thus, Fig. 6 shows how thermal stress is affected by an increasing number of parallel-connected strings (N_{pa} variable) for the worst case of thermal stress. In other words, the PVG was open-circuited with 79 PVMs short-circuited. The PVG did not have any BoDs. In simulations, performed at PTC, the PVG output power remained constant. Therefore, as parallel-connected strings increased, there was a proportional reduction of serial-connected PVMs in the strings.

Fig. 6 shows that if the PVG had more than four parallel-connected strings, the temperature reached in the PVM* was higher than its ST ($T_{\text{c ST}}$). The safe number of parallel-connected strings in the PVG in case of a short-circuit fault ($N_{\text{S pa}}$ variable) was 4. Thus, at PTC, a 5.43 p.u power could be safely dissipated by the PVM*, and its reverse current-carrying capacity was 3.02 p.u. It was also observed that the reverse current ($i_{\text{F string}}$) through the PVM* increased linearly with the N_{pa} variable. However, the rise in dissipated power (p_{c} –PVM*–) was greater since the PVM* was forced to operate at increasing voltage (beyond its open-circuit voltage) as the N_{pa} variable increased. This caused the t_{ST} variable associated with the PVM* to decrease significantly.

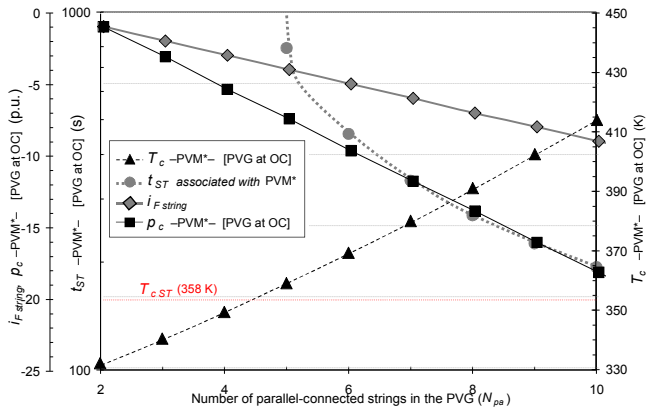

Figure 6. Thermal stress in the PVM* of the functioning 68-kWp PVG as a function of the Npa variable (worst case of thermal stress at PTC).

Because the temperature reached in the PVM*, in addition to the N_{pa} variable, depended on weather conditions, the simulations in Fig. 6, which maintained 80 serial-connected PVMs per string, were extended to several levels of irradiance and temperature, as said in the previous section. As a simulation result, Fig. 7 shows the safe number of parallel-connected strings in the PVG in case of a short-circuit fault ($N_{S\,pa}$ variable) as a function of weather conditions. For each $N_{S\,pa}$ value, the associated safe values of the reverse current ($i_{F\,string}$) and dissipated power for the PVM* (p_c (PVM*)) are also reflected.

It can also be observed how increasing irradiance produced a corresponding increase in absorbed solar power in the PVM*. This reduced its capacity to safely dissipate electrical power from the parallel-connected strings and also diminished its reverse current-carrying capacity. When the ambient temperature was higher, the potential thermal difference in the PVM* was smaller since the previously mentioned capacities again decreased. Low irradiances permitted high values of the $N_{S\,pa}$ variable since the current provided by each parallel-connected string was low. In contrast, rising temperatures produced smaller thermal differences, and thus lower values of the $N_{S\,pa}$ variable.

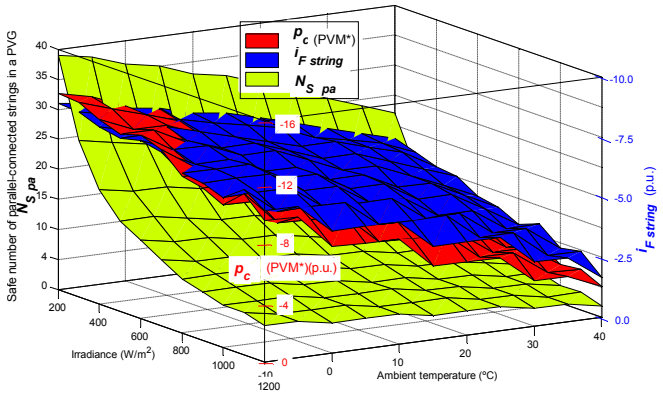

Figure 7. NS pa variable and its associated safe values of reverse current and dissipated power for the PVM* as a function of weather conditions in the functioning 68-kWp PVG without BoDs (vf = 1 m/s).

It is important to highlight that the reverse current-carrying capacity of the PVM* or its capacity to safely dissipate electrical power depended on weather conditions. This result is crucial for the definition of PVM overcurrent protection. Thus, since these capacities must be verified by applying a standard test [13], [14], [32], this test should be performed at adverse weather conditions [33].

B. *PVG Operating under an Open-Circuit Fault*

For the discussion of the effects of an open-circuit fault, this fault type was considered in a PVG string. Different degrees of severity were simulated (Fig. 8) by means of a series resistance in the faulty string which ranged from 0.001 to 5kΩ. BoDs did not influence PVG thermal results.

Fig. 8 shows the i–v_G characteristics of the faulty string and the PVG. Moreover, this figure shows the p_G–v_G characteristics and T_c–v_G characteristics for cells of PVMs belonging to the faulty string. The open-circuit fault considerably modified the faulty string i–v_G characteristic. Obviously, its extension depended on the resistance value, and caused it to become almost a straight line. The i_G–v_G characteristic changed as well, though to a lesser extent, depending on the number of parallel-connected strings in the PVG (N_{pa} variable). There were no problems of thermal stress since the PVMs of the faulty string were being disabled as series resistance increased.

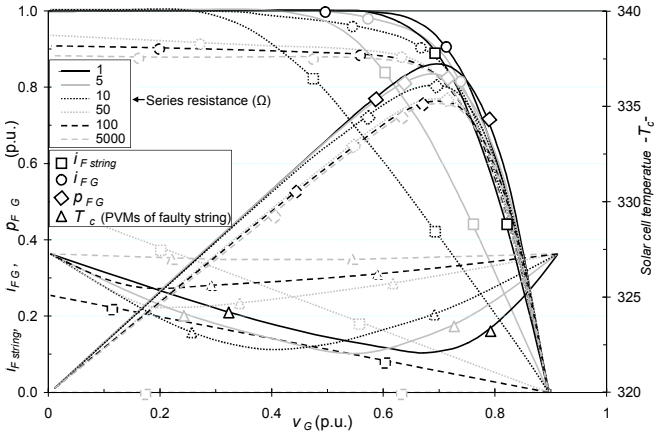

Figure 8. Simulation results for different characteristics in the functioning 68-kWp PVG at PTC, with an open-circuit fault in a string.

C. *PVG Operating under a Distributed Earth Fault*

To illustrate the effects of this fault type, we analyzed several cases of increasing severity for a uniform distributed earth fault in the PVG. Concretely, the PVG insulation resistance ($R_{iso\,G}$) was set at 1000kΩ, 100, 10, 1Ω. PVG leakage capacitance ($C_{lek\,G}$) and the F parameter (R_p/R_s) were always set at 46μF and 70 times, respectively [31]. BoDs were irrelevant since they did not influence PVG thermal results.

Earthed PVG at the negative terminal was the worst-case distributed earth-fault scenario from perspective of thermal stress. When the floating PVG was simulated, nearly one order of magnitude lower for $R_{iso\,G}$ was necessary, in relation to earthed PVG, to obtain equivalent results.

In Fig. 9 the PVM closest to the positive terminal dissipated power in the form of heat because of its insulation resistance. Thus, the dissipated power by the insulation resistance at cell level ($p_{D\,iso\,c}$ variable) was negative. However, this PVM did not become reverse biased (p_{mod}>0 p.u.). This low dissipated power slightly increased the module temperature, but the temperature always remained lower than its ST. The maximum temperature occurred when the PVG was open-circuited. Dissipated power and temperature increased with the reduction in PVG insulation. But, the increase was less in the case of PVMs as they were closer to negative one.

Significant changes occurred when PVG insulation was

lower than about 100 Ω. This value is much lower than the 100 kΩ minimum insulation resistance for this PVG [5].

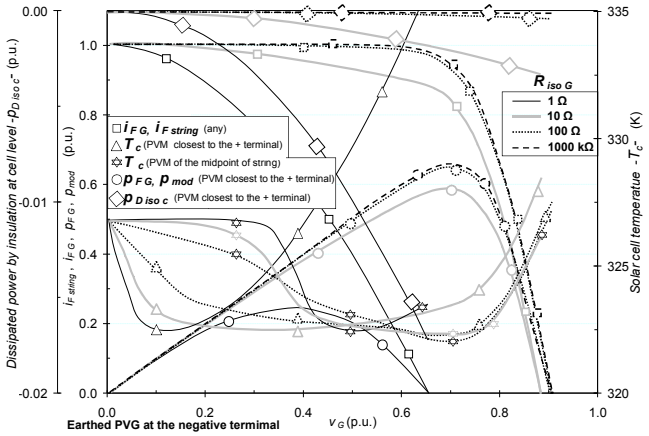

Figure. 9. Simulation results for different characteristics in the functioning 68-kWp PVG (negative terminal to earth) at PTC, changing its insulation.

D. Summary of Critical Observations of the PVG Operation under Electrical Fault

When there are BoDs in the short-circuit there are no thermal stress problems for PVMs. However, if BoDs are omitted, the destruction of PVMs due to thermal stress is possible. The thermal stress is dependent on various parameters, such as PVG configuration, number of PVMs short-circuited, and weather conditions.

The open-circuit fault and distributed earth fault are not a source of thermal stress problems for PVMs.

IV. Experimental Investigation of Electrical Faults on a PVG

The results of this research confirmed previous simulation results and consequently validated the simulation model used. The test was carried out on a functioning 68-kWp PVG [28] in nearly stable weather conditions in order to highlight solely the effects of electrical faults. The PVG was forced to operate from OC to Short-Circuit (SC) conditions with different electrical faults simulated by additional switches. Thus, our experiment included the following stages (Fig. 10): *i)* a twenty-module segment of one of the PVG strings was short-circuited when the PVG operated in MPP conditions, *ii)* the segment was extended to forty PVMs and *iii)* the PVG was open-circuited, and then subsequently short-circuited in the short-circuit electrical fault condition. All-important PVG variables (e.g. faulty/non-faulty string currents and voltages) as well as weather conditions and the cell temperature of the different PVMs were recorded during the experiment.

The short-circuit of 20 PVMs in a string (at t= 200 s) decreased the PVG voltage at MPP conditions. This caused the PVG output power to shift from 0.61 p.u. to 0.56 p.u. The PVMs* did not dissipate power since the PVG operated at MPP conditions. Nevertheless, their temperature increased slightly because their output power decreased by almost half. The short-circuit of 40 PVMs (at t= 300 s) decreased the PVG voltage at MPP conditions even more (about 0.49 p.u.). However, the PVG could not reach this MPP voltage, and was thus forced to operate at 0.62 p.u., the minimum MPP voltage of the PV inverter. With this PVG voltage, the PVMs* dissipated power. This significantly increased their temperature, causing it to rise exponentially. The increase in cell temperature decreased the PVG current since its voltage could not change. At t= 700 s, when the PVG was open-circuited, the cell temperature in PVMs* increased more powerfully. In fact, this temperature reached ST in 99 s. The PVG was short-circuited at t= 799 s so as not to damage the PVMs*. While the PVG did not yield power (SC or OC conditions), the cell temperature in the PVMs of the non-faulty strings increased. However, this increase that was observed until 700 s was only caused by weather conditions.

We found that simulated results closely matched experimental values, and, thus validated our model.

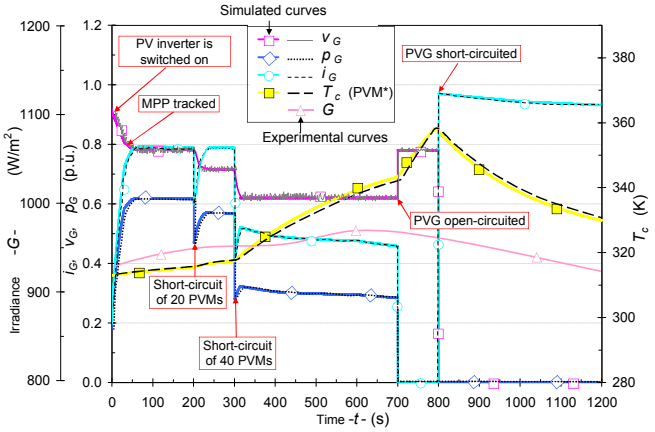

Figure 10. Simulation and experimental results on the test setup: functioning 68-kWp PVG.

V. PVG-Adapted Protective Measures against Overcurrent

Fundamental principles of protection for safety in LV electrical installations [4] demand that persons and property will be protected against the harmful effects of any overcurrent likely to arise in live conductors due to faults. These effects include mechanical stress and excessive temperatures, which are likely to cause burns, fires, and other harmful events.

Although PVMs are current-limited power sources, an overcurrent may appear in parallel-connected strings/arrays, and/or the utility grid in the event of faults to earth or between live parts in the PVG. More specifically, the overload is caused by resistive faults whereas short-circuits are due to zero/low resistance faults.

This section presents the optimal requirements for the protection of live parts in PVGs (i.e. line conductors and PVMs) from the effects of overcurrents. These requirements are modifications, adaptations, or reelaborations of the general requirements for AC LV installations [26] as well as of the more specific requirements for PV systems [30]. Since PVMs are part of the installation, the protection of line conductors in [26] is also extended to PVMs.

A. Limitation of Overcurrent by Characteristics of Supply

This measure entails limiting the maximum overcurrent to a safe value. Under this protective measure, the overcurrent is supplied by a source incapable of feeding a current exceeding the conductor's current-carrying capacity and the PVM's reverse current-carrying capacity (e.g. PV strings/arrays). The PV inverter must thus no be capable of back feeding utility currents into the faults of the PVG [34], [35]. A battery storage system is disallowed.

B. Protection by Automatic Disconnection of Supply

1) Requirements based on the nature of the circuit

Detection of any overcurrent in a PVG may be carried out at a single point of the PVG if electrical faults between its live parts can be discounted [5]. Thus, fault current can be detected at the earth connection of an earthed PVG. In contrast, an insulation monitoring device (IMD), connected to the PVG negative terminal, detects the resistance reduction caused by a fault in a floating PVG.

When it is necessary to perform an over-current discrimination (e.g. overcurrent detection at PV string/array/DC-main cable level), detection is usually provided on only one live conductor of the relevant circuit (string/array/DC-main) [17]. Nevertheless, overcurrent detection is provided in both positive and negative cables in floating PVGs to take into account the double earth fault [17]. In any case, detection causes the disablement of the PV string/array or PVG in which the overcurrent is detected.

In earthed PVGs, there is no need to provide overcurrent detection for the earthing conductor (bonded to the negative live conductor or centre-tap of the PVG [5]) since its cross-sectional area is usually equal to that of the line conductors.

2) Nature of PDs

Overcurrent PDs for PVGs must be different from the conventional ones for AC LV systems. On the one hand, these conventional overcurrent PDs (fuses and circuit-breakers) may not clear faults in a PVG since its limited current depends on weather conditions. On the other hand, the procedure used for the automatic disconnection of supply in AC LV systems (opening of the protected circuit) is not valid in PVGs for reasons of personal safety [5], [36]. Therefore, an alternative shutdown procedure is proposed in [5]. This shutdown procedure short-circuits and bonds the live conductors to earth at the inverter DC input, which has been previously separated from the DC side.

The coordination required between overcurrent and electric shock protection affords the possibility of using the same PD for both protections. The proposed PD against electric shock [5] has overcurrent PD functions, i.e. fault detection and PVG disablement. Thus, this PD has a detection/evaluation unit (monitoring device), which, in turn, triggers another device that disables the PVG (shutdown system). The monitoring device is a residual current monitor (RCM) [37] for earthed PVGs and an IMD [38] for floating PVGs [5]. Nevertheless, this PD operating as an overcurrent PD globally disables the PVG, involving low over-current discrimination. Disablement at PV array/string level is possible, but it requires more hardware with higher costs and higher potential failure rates. The use of this combination of devices provides the same level of protection as that of fuses and circuit-breakers [26].

The overcurrent PD proposed only detects earth faults, whereas faults between live parts are not detected. Therefore, in order to be able to discount line-to-line faults the PVG wiring must be laid in such a way that the likelihood of the occurrence of a fault between live parts is virtually reduced to zero. The code [39] lists various types of short-circuit-proof wiring, which practically exclude the occurrence of line-line faults. PVG requirements include laying separate wires for plus and minus, either by using single-core sheathed cables in separate cable ducts or cables with double or reinforced insulation [12]–[14], [17], [30]. This special wiring should be applied throughout the PVG. This includes the wiring of junction boxes and DC LV switchboards and panel boards. Additionally, class II PVMs [33] are also recommended.

3) Protection against overload current

Since there is a single shutdown system for the whole PVG, the overcurrent PD ensuring protection against overload only has a single monitoring device. The position of this monitoring device changes depending on the type of earthing system of the PVG. Thus, an RCM is installed in the earthing conductor for earthed PVGs, and an IMD is set up between the negative terminal and earth for floating PVGs [5]. When the monitoring device is designed to detect faults in PVG subsystems (e.g. PV string/array), a shutdown system for each PVG subsystem must be installed in order to achieve higher over-current discrimination.

Regarding the operating characteristics of the overcurrent PD protecting the PVG wiring and PVMs against overload, the monitoring device should satisfy different conditions, depending on the earthing system of the PVG.

In earthed PVGs, the RCM set point ($I_{\Delta n}$) that triggers the PVG shutdown system must satisfy:

$$0.5 \cdot I_{\Delta n} \geq I_{lek\ G\ \max} >> I_{Z\ i} \text{ (for all } ith \text{ PV DC circuits)} \quad (2)$$

where $I_{\text{lek G max}}$ is the maximum leakage current of the PVG and $I_{\text{Z i}}$ is the continuous current-carrying capacity of the *i*th circuit.

This trip level also affords personal protection [5].

In floating PVGs, the IMD set point (R_{an}) that triggers the PVG shutdown system must satisfy:

$$1.5 \cdot R_{an} \geq R_{iso\ G\ \min} \quad (3)$$

where $R_{\text{iso G min}}$ is the minimum insulation resistance of the PVG.

Again, this trip level also affords personal protection [5].

Moreover, in both earthing configurations, the following condition must be satisfied:

$$I_{B\ i} = 1.56 \cdot I_{SC\ i-STC} \leq I_{Z\ i} \text{ (for all } ith \text{ PV DC circuits)} \quad (4)$$

where $I_{\text{B i}}$ is the design current for the *i*th circuit (PV string/array) and $I_{\text{SC i–STC}}$ is the short-circuit current of the *i*th circuit at STC conditions.

4) Protection against short-circuit currents

Position of an overcurrent PD for short-circuit protection does not change in relation to the previously described one for overload protection since it is the same PD.

Regarding the operating characteristics of the overcurrent PD, breaking capacity is not a characteristic to take into account since the PVG shutdown system differs from the one in the AC LV system. Because PVG is a current-limited power source, the PVG maximum short-circuit current, increased by 1.56 times [9], must be taken into account when dimensioning the PVG shutdown system. When several shutdown subsystems are designed for PVG, their relevant currents must be taken into account. The previously defined set points of monitoring devices for overload protection guarantee short-circuit protection as well.

For the protection of wiring, the limit time (t_{limit} variable) to disable the PVG, in the case of a short-circuit, should not exceed the time needed to bring the insulation of the conductors to the permitted limit temperature. This time

may be calculated from:

$$t_{limit} = \min\left(\frac{k_i \cdot S_i}{I_{SC\ flow\ i\ \max}}\right)^2_{\text{for all } ith \text{ PV DC circuits}} \quad (5)$$

where $I_{SC\ flow\ i\ max}$ is the maximum short-circuit current flowing through the ith circuit/conductor due to short-circuits in the PVG, S_i is the cross-sectional area of the ith circuit, and k factor for ith circuit comes from Table 43A [26].

When the conductor's maximum current-carrying capacity ($I_{Z\ i}$) is twice its design current ($I_{B\ i}$), Equation 6, the limit time deduced from Equation 5 also guarantees protection of the PVMs. A PVM can withstand up to two times its reverse current in adverse weather conditions (G: 1000 W/m2, T_a: 40 ºC, v_f: 1 m/s, see section III.A.2):

$$I_{Z\ i} \le 2 \cdot I_{B\ i} \quad (6)$$

VI. Application of the Protective Measures against Overcurrent in a PVG

The protective measures against overcurrent for PVGs, according to [26], should be applied as follows: *i)* protection by limiting the supply of the overcurrent and *ii)* protection by automatic disconnection of supply.

Since the first protective measure guarantees overcurrent protection through PVG design (preventive measure), this measure is regarded as "passive". In contrast, the second measure is considered to be "active" because protection depends on PDs that operate when risk scenarios appear.

The choice of overcurrent protection is determined by PVG arrangement (serial-parallel configuration), installation location (accessibility, construction materials), skill level of maintenance team, cost of protective hardware, and PVG availability. These aspects, as well as others, should also be considered in the definition of electric shock protection [5] and lightning and surge protection [6] (other important safety issues). Consequently, it is necessary to agree on a safety design. When it is only a question of overcurrent protection, the following options are possible.

A. Protection by Limiting the Supply of Overcurrent

This protective measure is advisable for PV power applications with a low number of parallel-connected strings, and without a battery storage system.

The maximum number of strings that can be connected in parallel depends on both the conductor's current-carrying capacity and the PVM's reverse current-carrying capacity. The former is a function of the cable type used, its cross-section, and type of wiring system [39]. The latter depends on the prospective maximum ambient temperature and irradiance. According to section III.A.2, for example, the reverse current-carrying capacity of a specific PVM ranged from 1.42 p.u. to 7.52 p.u.

B. Protection by Automatic Disconnection of Supply

This protective measure is advisable for PV power applications with a medium-high number of parallel-connected strings.

The floating PVG (the safer option) offers clear advantages for avoiding fire and other safety risks. Two earth faults are required for the risk to exist against only one fault in earthed PVGs. Therefore, a floating configuration is advised for crowded sites or sites with easy accessibility, whereas an earthed PVG is advisable for areas with little traffic and non-specialized maintenance personnel.

VII. Conclusion

This paper provides a description and discussion of theoretical concepts, the use of models, and the adaptation of standard IEC 60364-4-43 requirement [26] to achieve overcurrent protection in PVGs.

The PVG model developed in [1], [2] allowed us to determine that although there were three types of potential electrical faults because of overcurrents, only the short-circuit fault could originate thermal stress problems in PVMs and PVG wiring. Therefore, some sort of overcurrent protection was required. The magnitude of thermal stress in PVMs was found to depend on the PVG configuration and the number of PVMs short-circuited, besides other commonly known factors, such as weather conditions.

A field test on our functioning 68-kWp PVG of the Univer Project [28] proved the accuracy of simulation results, regarding risk due to overcurrents. This validated the simulation model used in our study and the results obtained with it.

Regarding the overcurrent protection requirements in PVGs, this research study performed in a functioning 68-kWp PVG substantially clarified the application of the IEC 60364-4-43 requirements in PVGs. It was found that certain measures could be usefully applied; some needed to be specifically adapted to PV operating characteristics; and others were not applicable. The discussion of the results in this paper provides an adapted set of design rules which are basic guidelines for overcurrent protection in PVG.

Overcurrent protection by automatic disconnection of supply in floating configurations was selected for this study. This choice, which included the suppression of BoDs and fuses in strings/arrays, led to a simpler and more reliable PVG. PVG availability increased as a result of this design. Any electrical fault was immediately detected and communicated to the maintenance team. Short-circuit-proof wiring and the use of class II PVMs practically excluded the occurrence of line-line faults. Furthermore, the use of the same PD for electric shock and overcurrent protection eliminated any negative interference between both protections. The effectiveness of this PD was proved in [5].

References

[1] O. G. García, J. C. Hernández, F. Jurado, "Assessment of Shading Effects in Photovoltaic Modules," in: *Proc. 2011 Asia-Pacific Power and Energy Engineering Conference*, Wuhan, Mar. 2011, pp. 1–4. [Online]. Available: http://dx.doi.org/10.1109/APPEEC.2011.5747719

[2] J. C. Hernández, O. G. Garcia, F. Jurado, "Photovoltaic Devices under Partial Shading Conditions," International Review on Modelling and Simulations, vol. 5, no.1, pp. 414–425, Feb. 2012.

[3] D. L. Loveday, A. H. Taki, "Convective Heat Transfer Coefficients at a Plane Surface on a Full-Scale Building Façade," International Journal of Heat and Mass Transfer, vol. 8, no. 39, pp. 1729–1742, May. 1996. [Online]. Available: http://dx.doi.org/10.1016/0017-9310(95)00268-5

[4] IEC Std. 60364-1, "LV Electrical Installations - Fundamental Principles, Assessment of General Characteristics," IEC, 2005.

[5] J. C. Hernandez, P. G. Vidal, "Guidelines for Protection against Electric Shock in PV Generators," IEEE Transactions on Energy Conversion, vol. 24, no. 1, pp. 274–282, Mar. 2009. [Online]. Available: http://dx.doi.org/10.1109/TEC.2008.2008865

[6] J. C. Hernandez, P. G. Vidal, F. Jurado, "Lightning and Surge Protection in Photovoltaic Installations," IEEE Transactions on Power Delivery, vol. 23, no. 4, pp. 1961–1971, Oct. 2008. [Online]. Available: http://dx.doi.org/10.1109/TPWRD.2008.917886

[7] D. E. Collier, T. S. Key, "Electrical Fault Protection for a Large Photovoltaic Power Plant Inverter," in: *Proc. 20th IEEE Photovoltaic Specialists Conference*, Las Vegas, Sept. 1988, pp. 1035–1042. [Online]. Available: http://dx.doi.org/10.1109/PVSC.1988.105863

[8] T. Key, D. Menicucci, "Practical Application of the National Electrical Code to PV System Design," in: *Proc. 20th IEEE Photovoltaic Specialists Conference*, Las Vegas, Sept. 1988, pp. 1110–1115. [Online]. Available: http://dx.doi.org/10.1109/PVSC.1988.105877

[9] ANSI/NFPA-70-Article 690, "National Electrical Code –Solar PV Systems," National Fire Protection Association, 2008.

[10] M. Moechtar, M. Syafry-Syarief, Y. Effendi, "The Function of a Ground Sensor for Photovoltaic System Reliability," Renewable Energy, vol. 1, no. 2, pp. 177–182, 1991. [Online]. Available: http://dx.doi.org/10.1016/0960-1481(91)90073-X

[11] S. J. Durand, D. Bowling, V. V. Risser, "Lessons Learned from Testing Utility Connected by PV Systems," in: *Proc. 21th IEEE Photovoltaic Specialists Conference*, Kissimimee, May. 1990, pp. 909–913. [Online]. Available: http://dx.doi.org/ 10.1109/PVSC.1990.111752

[12] W. Wiesner, W. Vaaβen, F. Vaβen, "Safety Aspects for Installation and Operation of Grid Connected Photovoltaic Plants," in: *Proc. 11th EU PVSEC*, Montreux, Oct. 1992, pp. 1463–1067.

[13] H. Laukamp, "The Basic German Electric Safety Standard and its Application to PV Systems," in: *Proc. 12th EU PVSEC*, Amsterdam, Apr. 1994, pp. 1868–1872.

[14] H. Laukamp, G. Bopp, "Residential PV Systems Electrical Safety Issues and Installation Guidelines," Progress in Photovoltaics: Research and Applications, vol. 4, pp. 307–314, Jul. 1996. [Online]. Available: http://dx.doi.org/10.1002/(SICI)1099-159X(199607/08)4:4<307::AID-PIP134>3.0.CO;2-I

[15] R. Hotopp, K. Jaeger-Hezel, "On the Possibilities to Avoid Series Blocking Diodes and Bypass Diodes," in: *Proc. 12th EU PVSEC*, Amsterdam, Apr. 1994, pp. 1678–1681.

[16] J. Wiles, "Photovoltaic power systems and the 2005 national electrical code: suggested practices," Nov. 2008.

[17] IEC Std. 62548, "Solar Photovoltaic Energy Systems - Part 82/481/NP: Design Requirements for Photovoltaic (PV) Arrays," IEC, 2007.

[18] IEEE Std. 1374, "Guide for Terrestrial Photovoltaic Power System Safety," IEEE, New York, 1998.

[19] G. E. Ahmad, M. A. Mohamad, S. A. Kandil, R. Hanitsch, "Fault Detection in PV Generators Using an Improved Electronic Load," in: *Proc. 14th EU PVSEC*, Barcelona, Jun. 1997, pp. 199–202.

[20] D. Stellbogen, "Use of PV Circuit Simulation for Fault Detection in PV Array Fields," in: *Proc. 23th IEEE Photovoltaic Specialists Conference*, Louisville, May. 1993, pp. 1302–1307. [Online]. Available: http://dx.doi.org/10.1109/PVSC.1993.346931

[21] J. C. Wiles, D. L. King, "Blocking Diodes and Fuses in Low-Voltage PV Systems," in: *Proc. 26th IEEE Photovoltaic Specialists Conference*, Anaheim, Sep. 1997, pp. 1105–1108. [Online]. Available: http://dx.doi.org/10.1109/PVSC.1997.654281

[22] G. Nofuentes, J. C. Hernandez, G. Almonacid, J. M. Abril, "Analysis of the Possibilities to Omit Blocking and Bypass Diodes Using a Standard Circuit Simulator," in: *Proc. 14th EU PVSEC*, Barcelona, Jun. 1997, pp. 1094–1096.

[23] C. Bendel, E. Kunz, U. Rudolph, "Monitoring and Defect Diagnosis of PV Systems," in: *Proc. 2nd World Conference on Photovoltaic Solar Energy Conversion*, Vienne, Jul. 1998, pp. 2165–2168.

[24] J. C. Hernandez, G. Almonacid, "Development of a Fault Detection System in a PV Installation," in: *Proc. 2nd World Conference on PV Solar Energy Conversion*, Vienna, Jul. 1998, pp. 2131–2134.

[25] C. Kuei-Hsiang, L. Ching-Ju, H. Sheng-Han, "Modeling and Fault Simulation of Photovoltaic Generation Systems Using Circuit-Based Model," in: *Proc. 2008 International Conference on Sustainable Energy Technologies*, Singapore, Nov. 2008, pp. 290–294. [Online]. Available: http://dx.doi.org/10.1109/ICSET.2008.4747019

[26] IEC Std. 60364-4-43, "Low-Voltage Electrical Installations - Protection for Safety - Protection against Overcurrent," IEC, 2008.

[27] H. Laukamp, G. Boop, L. Niebers, "The Hazard of Electric Arcs in Residential PV Systems Assessment and Installation Guidelines," in: *Proc. 11th EU PVSEC*, Montreux, Oct. 1992, pp. 1444–1447.

[28] M. Drif, P. J. Pérez, J. Aguilera, G. Almonacid, P. Gómez, J. D. L. Casa, "Univer Project. A Grid Connected Photovoltaic System of 200 kWp at Jaén University. Overview and Performance Analysis," Solar Energy Materials & Solar Cells, vol. 91, pp. 670–683, Feb. 2007. [Online]. Available: http://dx.doi.org/10.1016/j.solmat.2006.12.006

[29] J. H. Boumans, A. J. N. Schoen, S. A. M. Verhoeven, "Test Facilities and Safety Regulations for Rooftop Mounted and Grid-Connected PV Systems," in: *Proc. 1st World Conference on Photovoltaic Energy Conversion*, Waikoloa, Dec. 1994, pp. 1024–1027. [Online]. Available: http://dx.doi.org/10 10.1109/WCPEC.1994.520135

[30] IEC Std. 60364-7-712, "Electrical Installations of Buildings - Requirements for Special Installations or Locations - Solar PV Power Supply Systems," IEC, 2002.

[31] J. C. Hernández, P. G. Vidal, A. Medina, "Characterization of the Insulation and Leakage Currents of PV Generators: Relevance for Human Safety," Renewable Energy, vol. 35, pp. 593–601, Mar. 2010. [Online]. Available: http://dx.doi.org/10.1016/ 10.1016/j.renene.2009.08.006

[32] W. Knaupp, "Standardization of Data Sheet and Nameplate Specifications of PV Modules," in: *Proc. 25th IEEE Photovoltaic Specialists Conference*, Washington, May. 1996, pp. 1303–1306. [Online]. Available: http://dx.doi.org/10.1109/PVSC.1996.564372

[33] IEC Std. 61730 series, "PV Module Safety Qualification," IEC, 2004.

[34] IEC Std. 62109-1, "Safety of Power Converters for Use in Photovoltaic Power Systems - General Requirements," IEC, 2010.

[35] IEC Std. 62109-2, "Safety of Power Converters for Use in PV Power Systems - Particular Requirements for Inverters," IEC, 2011.

[36] P. G. Vidal, G. Almonacid, P. J. Perez, "Measures Used to Protect People Exposed to a PVG: Univer Project," Progress in Photovoltaics: Research and Applications, vol. 9, pp. 57–67, Feb. 2001. [Online]. Available: http://dx.doi.org/10.1002/pip.348

[37] IEC Std. 62020, "Electrical accessories –Residual current monitors for household and similar uses (RCMs)," IEC, 2003.

[38] IEC Std. 61557-8, "Equipment for Testing, Measuring or Monitoring," IEC, 2007.

[39] IEC Std. 60364-5-52, "LV Electrical Installations - Selection and Erection of Electrical Equipment - Wiring Systems," IEC, 2009.